Journal of Inclusion Phenomena and Molecular Recognition in Chemistry **17:** 221–235, 1994.

Physicochemical Properties of Alkali-Metal Exchanged Type X Zeolites*

S. S. TAMHANKAR and V. P. SHIRALKAR**
National Chemical Laboratory, Pune – 411008, India.

(Received: 22 March 1993; in final form: 28 January 1994)

Abstract. The changes in the physicochemical properties of a series of faujasite type X zeolites cation exchanged with K^+, Rb^+ and Cs^+ have been studied by XRD, IR, thermoanalytical methods and sorption measurements. As a consequence of the enhanced scattering of X-rays by larger alkali metal cations, the percent relative intensity of the XRD peaks of cation exchanged zeolites was found to have decreased considerably. The framework IR spectra also showed analogous changes. The alkali metal exchange was found to enhance the thermal stability of the parent zeolite. The available void volume and specific surface area (obtained by low temperature nitrogen sorption) also decreased with the increase in the degree of exchange and cationic size. Equilibrium sorption capacities (298 K and $P/P_0 = 0.5$) for water, *n*-hexane, cyclohexane and 1,3,5-trimethylbenzene also exhibited the same trend.

Key words: Alkali metal exchanged X zeolites, structural, thermal and sorption properties.

Introduction

In consequence of their very open framework structure, faujasite type zeolites are extensively used [1] as catalysts for different hydrocarbon conversion reactions of industrial importance. Zeolite type X, exchanged with rare earths and/or protons, has been used as a cracking catalyst [2]. In addition to their usual acidic properties, base centres are formed in the framework of these zeolites when exchanged with K^+, Rb^+ Cs^+. Both acidic and basic centres in the zeolite framework have been recently reviewed by Barthomeuf [3]. Not only synthetic zeolites [4] but also a number of natural zeolites are modified by cation exchange [5] and consequently their sorption characters are also modified [6, 7]. Cesium- and rubidium-exchanged faujasite type zeolites have recently been used in side chain alkylation of the benzene ring [8]. The degree of cation exchange was found to be correlated with the catalytic activity. As a consequence of the cation exchange the physicochemical properties of the parent zeolites usually get modified. In the view of this we have systematically studied the physicochemical properties of type X zeolite cation exchanged with K^+, Cs^+ and Rb^+. The results are reported below.

* NCL communication no. 6056.
** Author for correspondence.

Experimental

MATERIALS AND METHODS

The binder-free zeolite was synthesised [9] using water-glass solution, sodium aluminate and sodium hydroxide. The SiO_2/Al_2O_3 mole ratio of the synthesised zeolite was found to be 2.52. K^+, Rb^+, Cs^+ exchanges were carried out at 368 K using 5% aqueous solutions of chloride salts of the respective alkali metal species, following the procedure reported elsewhere [10]. Samples with a higher degree of exchange were prepared by repeated cation exchange treatments. The chemical compositions of the parent and exchanged zeolites were determined by conventional wet gravimetric methods in conjunction with flame photometry (Toshniwal), atomic absorption spectrometry (Hitachi, Z8000) and inductively coupled plasma emission (ICPE) spectroscopy.

The changes in the crystallinity as a consequence of the cation exchange were examined from XRD patterns obtained on a Rigaku (model D-Max/III VC) diffractometer using Ni filtered CuK_α ($\lambda = 1.54041$ Å) radiation. The crystallinity was estimated from the intensities of some of the prominent peaks.

Framework IR spectra were recorded on a Pye-Unicam SP-300 spectrometer using the Nujol mull technique. DTA and TG curves were recorded simultaneously up to 1273 K on a Setaram 92-12 (France) thermal analyser in an air using precalcined α-alumina as a reference material.

Thermoanalytical curves were scanned with TG sensitivity = 30 mg and DTA sensitivity = 100 μV. Equilibrium sorption capacities (up to 2 h) were measured gravimetrically at 298 K ($P/P_0 = 0.5$) on a McBain–Baker-type apparatus using a silica spring balance. Prior to sorption measurements a 75 mg sample, pressed into a pellet, was activated at 673 K for 6 h under vacuum of 10^{-6} Torr.

The specific surface area of the sample was estimated by low temperature (78 K) nitrogen sorption using a BET volumetric apparatus, following the procedure described elsewhere [11].

Results and Discussion

UNIT CELL COMPOSITIONS OF THE CATION EXCHANGED ZEOLITES

Table I lists the unit cell compositions obtained from gravimetric chemical analysis of the exchanged samples. It can clearly be seen from Table I that during the cation exchange with aqueous salt solutions part of the Na^+ is replaced by H_3O^+, and therefore the actual number of cations exchanged by alkali metal is lower than the total cation exchange in terms of Na^+ removal. In aqueous cation exchange at pH around 4.5–5.0, Na^+ from the parent zeolite is exchanged by both H_3O^+ and M^+ ($M^+ = K^+$, Rb^+ and Cs^+). The composition at equilibrium depends upon the competition between H_3O^+ and M^+. Similar hydrolytic replacement of cations by H_3O^+ has also been reported in the literature [12]. It is also seen from Table I, that

TABLE I

Unit cell (u.c.) composition of the series of alkali metal cation exchanged type X zeolites.

Sample	Unit cell composition					Ion exchange $(H^+ + M^+)$ [%]	u.c., $g^{-1} \times 10^{-19}$
NaX		$Na_{90.7}$		$[(AlO_2)_{89.4}(SiO_2)_{102.6}]$	263.5 H_2O	–	4.46
HNaK(1)X	$H_{20.8}$	$Na_{42.0}$	$K_{29.8}$	$[(AlO_2)_{92.6}(SiO_2)_{99.34}]$	246.3 H_2O	55.8	4.44
HNaK(2)X	$H_{7.70}$	$Na_{20.2}$	$K_{64.4}$	$[(AlO_2)_{92.3}(SiO_2)_{99.71}]$	239.4 H_2O	77.7	4.18
HNaK(3)X	$H_{2.00}$	$Na_{14.3}$	$K_{72.3}$	$[(AlO_2)_{88.6}(SiO_2)_{103.4}]$	239.5 H_2O	83.4	4.13
HNaRb(1)X	$H_{12.7}$	$Na_{57.6}$	$Rb_{19.5}$	$[(AlO_2)_{89.8}(SiO_2)_{102.2}]$	243.0 H_2O	35.9	4.17
HNaRb(2)X	$H_{12.5}$	$Na_{42.4}$	$Rb_{33.8}$	$[(AlO_2)_{88.8}(SiO_2)_{103.2}]$	236.4 H_2O	52.3	3.93
HNaRb(3)X	$H_{11.1}$	$Na_{32.8}$	$Rb_{45.9}$	$[(AlO_2)_{89.8}(SiO_2)_{102.2}]$	232.2 H_2O	63.5	3.73
HNaCs(1)X	$H_{9.5}$	$Na_{57.6}$	$Cs_{22.7}$	$[(AlO_2)_{90.1}(SiO_2)_{98.9}]$	239.4 H_2O	36.1	3.81
HNaCs(2)X	$H_{9.50}$	$Na_{49.3}$	$Cs_{30.3}$	$[(AlO_2)_{89.1}(SiO_2)_{97.8}]$	299.0 H_2O	45.0	3.60
HNaCs(3)X	$H_{7.50}$	$Na_{37.3}$	$Cs_{49.8}$	$[(AlO_2)_{94.6}(SiO_2)_{97.3}]$	312.4 H_2O	60.6	3.18

$M^+ = K^+$ or Rb^+ or Cs^+.

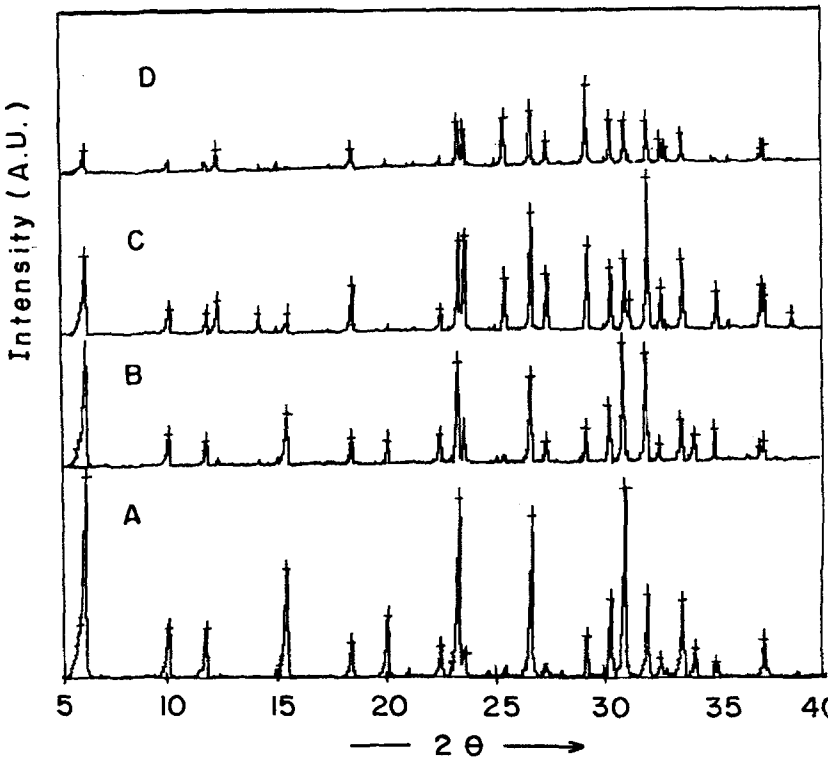

Fig. 1. XRD patterns for (A) NaX, (B) HNaK(3)X, (C) HNaRB(3)X, and (D) HNaCs(3)X.

on the basis of the unit cell compositions of the samples, the number of unit cells per gram also varies, depending on the atomic weight of the exchanged cation and degree of cation exchange.

X-RAY DIFFRACTION (XRD)

Table II summarises in detail the XRD characteristics of different cation exchanged zeolites. It shows a decrease in the relative intensities of the majority of XRD reflections and also an increase in that of some of the reflections. Figure 1 shows typical changes in the relative intensities of the parent NaX sample along with the samples of the highest degree of K^+, Rb^+ and Cs^+ cation exchange. Both Figure 1 and Table II show that the reflections most affected (i.e. decrease in the relative intensity) by progressive increase in the degree of cation exchange are the 111, 220, 331, 440, 533, 642 and 555 planes. The intensity of the plane 533 is reported [13] to be least affected by cation exchange. There is such a drastic decrease in the peak intensity of the 331 and 440 planes that they are almost absent in the HNaCs(3)X sample. A similar drastic decrease in the 220 and 331 planes was reported [14] in the case of rare earth-exchanged zeolite. The decrease in the peak intensity may

TABLE II

X-ray data for the series of alkali metal exchanged type X zeolite.

S*	474	316	273	266	305	223	201	143	121	81
hkl	NaX	HNaK(1)X	HNaK(2)X	HNaK(3)X	HNaRb(1)X	HNaRb(2)X	HNaRb(3)X	HNaCs(1)X	HNaCs(2)X	HNaCs(3)X
	% I/I_0									
111	100	58	57	58	65	39	39	19	19	11
220	25	19	19	16	19	18	13	12	9	–
311	24	13	13	8	18	13	10	11	10	10
331	54	33	26	26	24	13	9	–	–	–
333	17	17	16	13	25	29	23	12	11	09
440	30	21	12	12	8	–	–	–	–	–
620	15	14	13	14	10	13	10	6	–	–
533	89	69	56	51	67	53	45	36	31	22
622	11	22	19	18	41	50	47	21	21	18
642	81	57	46	43	67	61	59	42	35	27
733	20	19	17	17	33	43	43	34	36	40
660	39	34	29	29	33	31	31	20	18	22
555	95	59	57	60	55	39	35	34	27	21
840	41	53	51	55	64	75	76	31	27	21

* S = sum of the % relative intensities of the planes 111, 320, 331, 440, 533, 642, 555.

I_0 = Intensity of 111 plane in NaX = 100.

TABLE III. Framework (Al,Si–O) IR data for the series of zeolite products.

Zeolites	ν_{as}(T–O)	ν_s(T–O)	ν_s(O–T–O)		Zeolitic double ring D6R	(T–O) bend
NaX	1080	975	732	680	563	463
HNaK(1)X	1060	965	748	660	560	462
HNaK(2)X	–	970	750	680	555	455
HNaK(3)X	1067	962	740	665	560	462
HNaRb(1)X	1070	968	745	666	573	473
HNaRb(2)X	1051	978	740	666	569	471
HNaRb(3)X	1062	975	745	665	565	470
HNaCs(1)X	1073	963	730	680	563	456
HNaCs(2)X	1085	965	735	682	567	460
HNaCs(3)X	–	972	750	683	569	457

be, firstly, due to the higher scattering of X-rays on account of a comparatively larger size of incoming species and, secondly, on account of variations in cation site selectivity. The second possibility has also been supported by a surprising observation of an increase in the intensity of reflections corresponding to $2\theta = 26.0$ and 30.5. Another important observation is the appearance of additional peaks or a doublet in place of a singlet in HNaK(3)X, HNaRb(3)X and HNaCs(3)X samples, even after washing them thoroughly. The appearance of additional peaks leads either to a transformation of a lattice to a lower symmetry or to the occlusion of salts of K, Rb, Cs. When XRD data for the exchanged samples D, C and B from Figure 1 were analysed by a computer programme, it did not reveal any change to lower crystal symmetry. This suggests the occlusion of alkali halogenides (formed during cation exchange by alkali halides) in sodalite cages and hexagonal prisms formed through 6- and 4-membered rings.

FRAMEWORK IR SPECTRA

Framework IR spectra are listed in Table III along with the band assignments in accordance with the convention followed in the literature [15, 16]. A shoulder band around 1080 cm^{-1}, a strong band around 975 cm^{-1} due to the symmetric stretch [ν_s (T–O)], a doublet [ν_s (O–T–O)] around 740 cm^{-1} and 680 cm^{-1}, a band around 560–570 cm^{-1} due to the double six ring (D6R) and a band due to T–O bending deformation around 460–470 cm^{-1} are in close agreement with those reported in the literature [15]. All the exchanged samples from Table III do exhibit an IR band near the same positions (with slight changes in their position only in some cases). The change in the position may be due to the change in the mass numbers affecting the reduced masses in the evaluation of the force constant. The frequency of the shoulder band around 1080 cm^{-1} due to the asymmetric [ν_{as} (Al,Si–O)] stretch

TABLE IV. Thermoanalytical data for series of alkali metal exchanged type X zeolites.

Zeolitic product	m loss of H_2O (%)	DTA minima (K)	DTA end temp. for chemically sorbed water (K)	Si–Al lattice destruction (K)
NaX	22.63	449	700	1109
HNaK(1)X	21.42	–	642	1144
HNaK(2)X	20.98	450	689	1150
HNaK(3)X	20.20	449	700	1167
HNaRb(1)X	20.32	454	620	1141
HNaRb(2)X	18.84	459	621	1152
HNaRb(3)X	18.70	455	646	1160
HNaCs(1)X	19.20	454	610	1152
HNaCs(2)X	17.82	456	610	1169
HNaCs(3)X	16.00	454	607	–

varies in the range 1200–800 cm^{-1}. A strong band due to the symmetric stretch around 970 cm^{-1} varies in its position in the range 980–960 cm^{-1}. Similarly there is no definite trend with degree of exchange or with the nature of exchange cations in the frequency of a doublet around 750–680 cm^{-1}. It is found that the frequency decreases with an increase in the degree of exchange. This may be due to some dealumination [17] during ion-exchange treatment. Compositions of the ion exchanged samples listed in Table I do not account for significant dealumination. It is probable, therefore, that Al^{3+} knocked out during ion exchange becomes occluded in the solid as non-framework intrazeolitic species which are not removed after thorough washing, probably due to their occlusion in cages formed by 6- and 4-membered rings. This may be reflected in the enhanced thermal stability (discussed below) of the cation exchanged sample. The frequency of most of the bands including that due to (Od) T–O bend do not show any definite trend with the degree of exchange and the nature of exchanged cation.

THERMAL PROPERTIES

Usually the thermal properties are modified by different degrees of cation exchange with different extra-framework cationic species. The thermal properties of the series of alkali metals exchanged type X zeolite are summarized in Table IV.

TG curves showed that the desorption of physically sorbed water up to 460 K followed by the loss of hydroxyls and other forms of water up to 700 K in almost all cation exchanged zeolites. The temperature of complete dehydration was around 700 K in NaX; in KX series zeolites, however, it decreased in the RbX series to 645–620 K and in the CsX series to 610 K. The percentage loss in weight up to 700 K due to desorption of physically sorbed water (up to 460 K), hydroxyls and

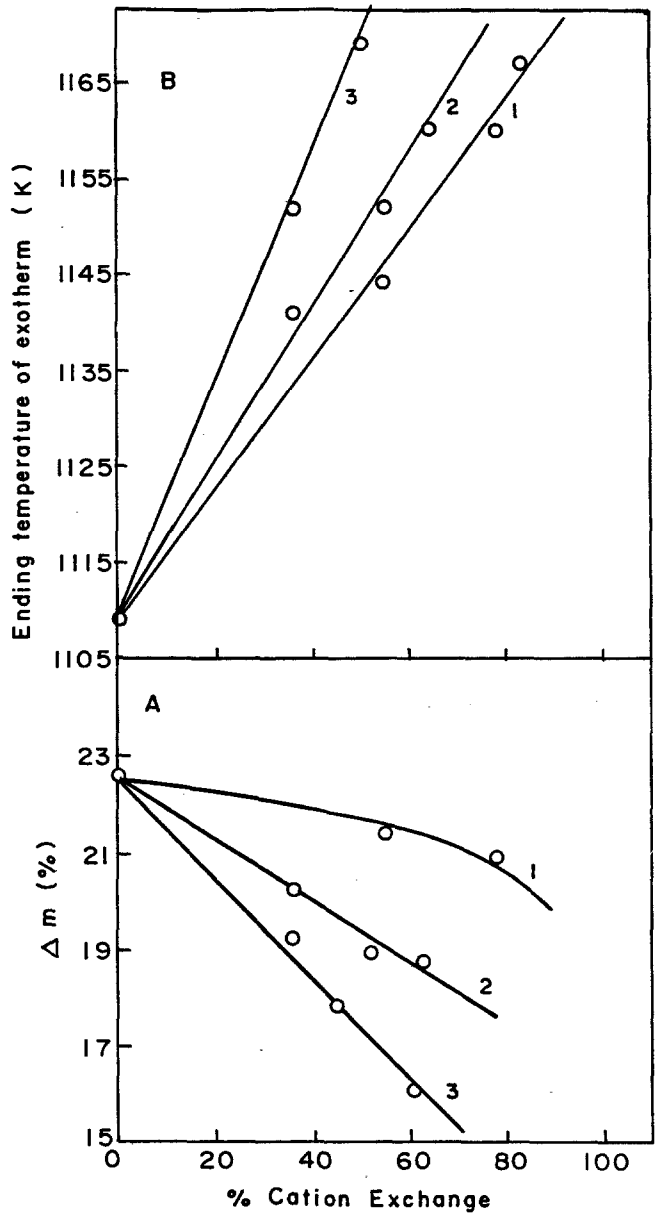

Fig. 2. Thermal properties of (A) wt.-% loss and (B) upper limiting temp. for exotherm (1) K^+ exchanged, (2) Rb^+ exchanged, and (3) Cs^+ exchanged type X zeolites.

other forms of water decreases with the degree of alkali metal exchange in zeolites. It decreases from 22.63 wt.-% for NaX to 20.2 wt.-% in HNaK(3)X to 18.7 wt.-% in HNaRb(3)X and to 16.0 wt.-% in HNaCs(3)X. Figure 2A shows the systematic decrease in the percentage loss in weight due to dehydrations in different alkali

TABLE V. Surface area and void volumes of the series of alkali metal exchanged type X zeolites.

Zeolite	Void volume (mL, g^{-1})			Surface area (m^2, g^{-1})	
	Dubinin	BET	Langmuir	Langmuir	BET
NaX	0.35	0.32	0.35	998	925
HNaK(1)X	0.32	0.29	0.32	912	834
HNaK(2)X	0.31	0.28	0.30	870	805
HNaK(3)X	0.30	0.28	0.30	860	794
HNaRb(1)X	0.30	0.27	0.29	831	765
HNaRb(2)X	0.29	0.25	0.28	799	721
HNaRb(3)X	0.26	0.25	0.26	742	705
HNaCs(1)X	0.27	0.24	0.27	771	683
HNaCs(2)X	0.26	0.22	0.25	730	636
HNaCs(3)X	0.23	0.20	0.23	648	587

metal exchanged type X zeolites. The decrease in the amount of physically sorbed water up to 460 K in cation exchanged type X zeolites is due to the larger cationic size of incoming cations compared to that of Na^+ and thus it leads to a reduction in the void volume available for sorption. All the DTA curves were characterized by a broad low temperature endotherm around 460 K due to the desorption of physically sorbed water. The temperature of the minimum of the endotherm may be taken qualitatively as a measure of the strength of a physical bond between sorption centres and extra-framework cations i.e. Na^+, K^+, Rb^+ and Cs^+. The temperature of the minimum of the endotherm shifts slightly to higher temperature from 449 K in NaX to 460 K in HNaRb(2)X. This demonstrates the comparatively stronger bonding of water molecules in RbX and CsX. Another striking feature of the DTA curves is the small but sharp high temperature exothermic process (usually considered [18] as a measure of thermal stability or the breakdown temperature of the zeolite lattice). It is seen from Table IV that the end temperature of the exotherm increases from 1109 K for NaX to 1167 K for HNaK(3)X, in the KX series and to 1160 K for HNaRb(3)X in the RbX series and the exothermic process not ending up to 1273 K in HNaCs(3)X. Figure 2B shows a systematic increase in the thermal stability of alkali metal exchanged type X zeolite. The increase in the thermal stability of these exchanged zeolites may be due to possible dealumination taking place during cation exchange. Alternatively, the increased basic character of the exchanged zeolite from Na^+ to Cs^+ may also be responsible for the increased thermal stability of the zeolite.

SORPTION PROPERTIES

The modification brought about in the zeolite voids on account of the cation exchange are usually studied by sorption of different molecules whose critical

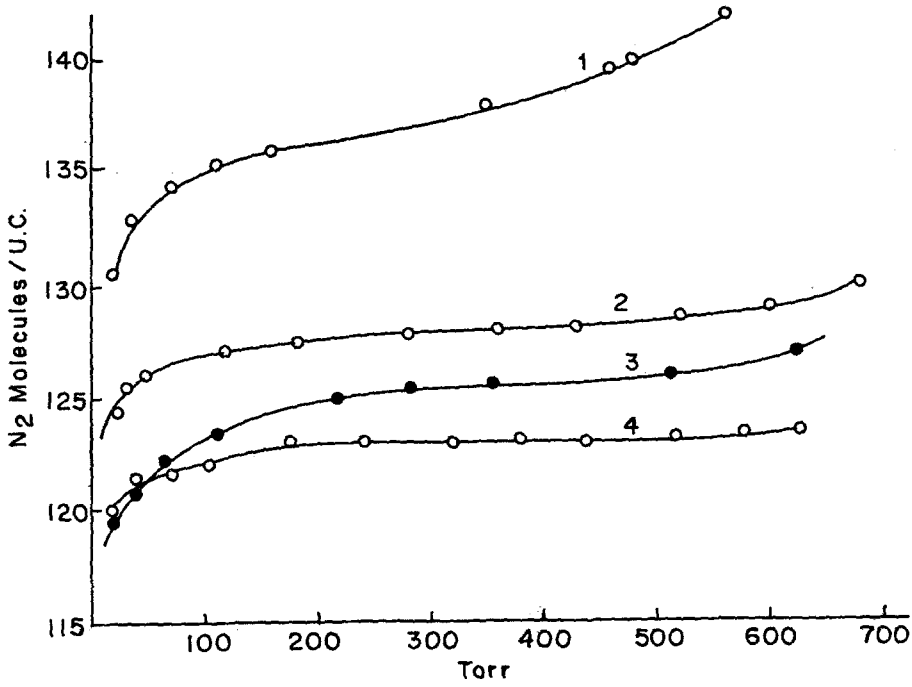

Fig. 3. Nitrogen sorption isotherms at 78 K in (1) NaX, (2) HNaK(3)X, (3) HNaRb(3)X, and (4) HNaCs(3)X.

diameter is comparable or lower than the pore opening of the zeolite lattice. Low temperature (78 K) nitrogen sorption helps to estimate the specific surface area and consequently the void volume of different cation exchanged zeolites. Low temperature nitrogen sorption isotherms in typical cation exchanged type X zeolites and zeolite NaX are shown in Figure 3. Isotherms for cation exchanged zeolites approach more towards the Langmuir model. Table V lists the specific surface areas of the cation exchanged samples from the low temperature nitrogen sorption data by applying the BET and Langmuir sorption models. Table V also lists the void volume obtained by applying the Dubinin–Radushkevich equation [19] along with the BET and Langmuir models. It has already been reported [20] that the Langmuir equation yields linear plots over a wide range of relative pressure (0.75) whereas the BET plots were linear over a narrow range of relative pressure (0.15). This is in accordance with the logical expectation of the lower probability of the multilayer formation in the zeolite voids based on which the BET model is derived; on the other hand, monolayer formation seems to be likely in the zeolite voids. The BET surface areas decrease from 925 $m^2\ g^{-1}$ for NaX to 794 $m^2\ g^{-1}$ for HNaK(3)X, to 705 $m^2\ g^{-1}$ for HNaRb(3)X, and to 587 $m^2\ g^{-1}$ for HNaCs(3)X. Void volumes also follow the same trend. The BET void volume decreases from

0.32 mL g^{-1} for NaX to 0.20 mL g^{-1} in HNaCs(3)X. The Langmuir void volume also decreases from 0.35 mL g^{-1} for NaX, to 0.23 mL g^{-1} in HNaCs(3)X. The Dubinin void volume is higher than both the Langmuir and the BET void volume. The Dubinin equation takes account of the drop in surface potential with the progressive increase in the surface coverage and Dubinin plots were found to be linear up to a relative pressure of 0.8. Multilayer formation and/or condensation at higher relative pressure (> 0.85) may lead to higher estimation of the void volume obtained by the extrapolation of the Dubinin plot. Figure 4 shows the systematic decrease in both the Dubinin void volumes and BET surface areas with the increase in the degree of alkali metal exchange and also with the increase in the size of alkali metal species. The cation site selectivity might have also caused the decrease in the available void volume in the framework of different alkali metal exchanged type X zeolites.

CHEMICAL POTENTIAL/SORPTION SELECTIVITY

A decrease in the chemical potential takes place when a gas at a standard pressure P_0 is transferred reversibly and isothermally into an infinite amount of sorbate–sorbent mixture over which the equilibrium pressure is P. If the nonideality of the gaseous sorbate, like nitrogen, is neglected, the chemical potential may be expressed as [21]:

$$\Delta\mu = RT \ln (P/P_0)$$

The value of $\Delta\mu$ is taken [22] as the measure of the chemical potential of the sorbate at the sorbent surface. Also at the fixed equilibrium pressure the measure of the chemical potential provides the sorption selectivity of a particular sorbent. Figure 5 exhibits systematic variation in the chemical potential as a function of coverage for nitrogen sorption in different alkali metal exchanged type X zeolites. It is seen from Figure 5 that the chemical potential decreases with the increase in the degree of exchange with alkali metal ions. The sorption selectivity follows the sequence NaX > HNaK(1)X > HNaK(2)X > HNaK(3)X > in a typical series and NaX > HNaK(3)X > HNaCs(3)X > HNaRb(3)X. In general, the chemical potential decreased with the amount sorbed and the decrease was much sharper in the higher coverage region, probably on account of condensation or multilayer formation. Similar results have been reported [20]for RE^{3+}, La^{3+}, and Ca^{2+} exchanged zeolites of faujasites.

EQUILIBRIUM SORPTION CAPACITIES

The modifications brought about in the void volumes of different framework zeolites are also studied by equilibrium sorption capacities of probe molecules of different sizes and polarities. Sorption of comparatively smaller and polar molecules like water helps to determine the hydrophilic and/or hydrophobic character of the

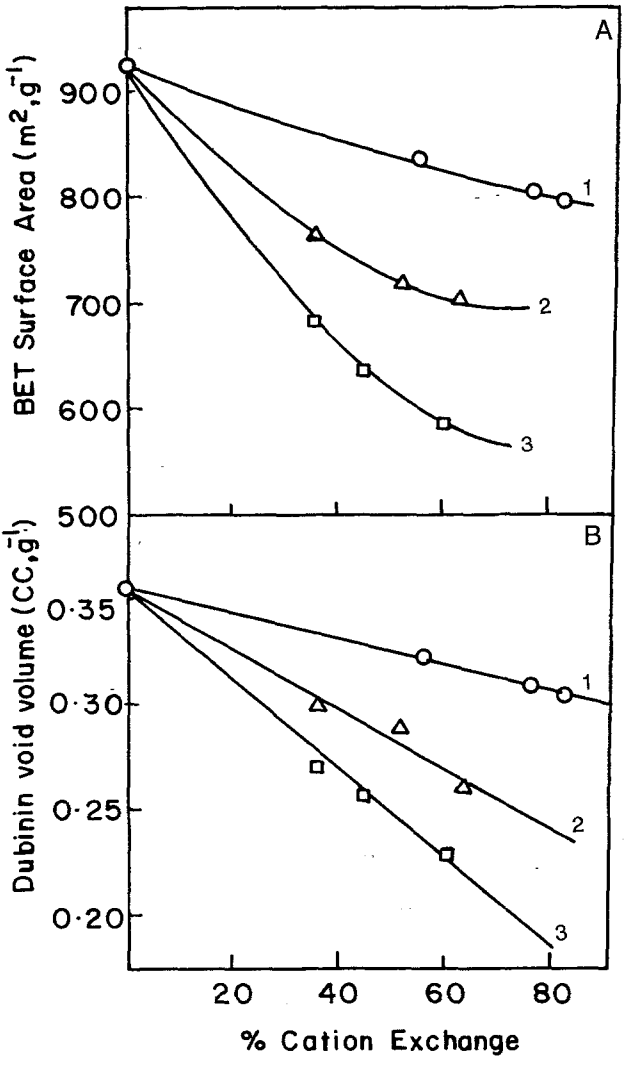

Fig. 4. Change in BET surface area (A) and Dubinin void volume, (B) in (1) K^+ exchanged, (2) Rb^+ exchanged, and (3) Cs^+ exchanged type X zeolites.

zeolite framework as well as the extent of aluminum incorporation in the solid. n-Hexane, being a non-polar, cylindrical molecule gives the measure of the total void volume of the zeolite. Unlike water, n-hexane, however, cannot penetrate the polyhedralike hexagonal prism and sodalite cage (β cage) on account of the smaller size of their entry windows. Similarly benzene, cyclohexane and 1,3,5 trimethyl-benzene (TMB), with still larger molecular sizes, give a measure of changes only in the supercage (α-cage) cavities. Figure 6 represents the kinetics of sorption of water, n-hexane, benzene and cyclohexane in a typical series of alkali metal

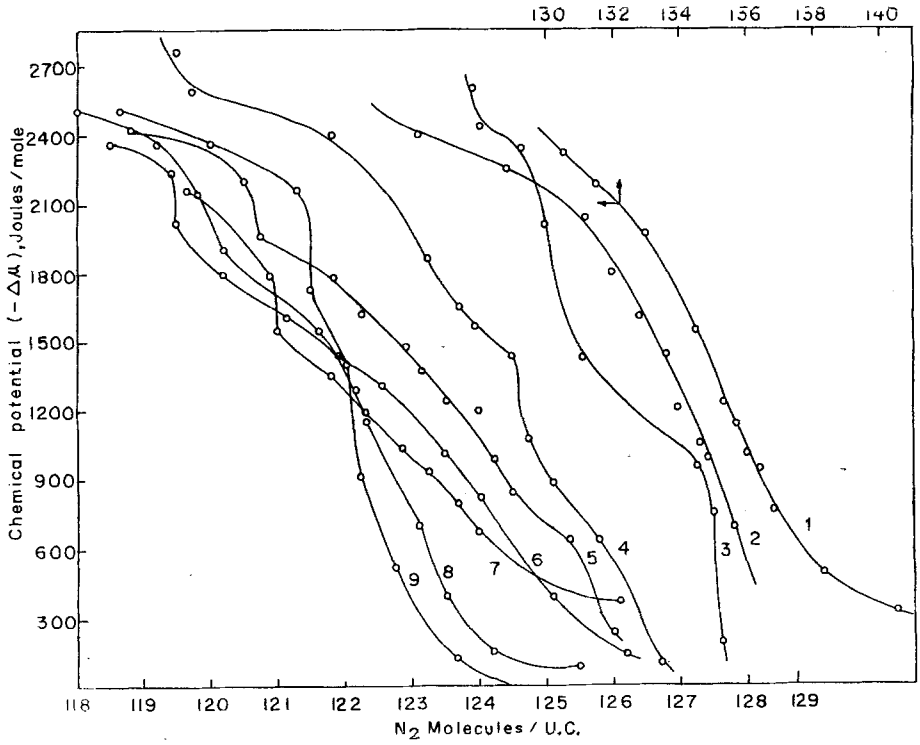

Fig. 5. Variation in chemical potential $(-\Delta\mu)$ with the amount of nitrogen sorbed in (1) NaX, (2) HNaK(3)X, (3) HNaK(2)X, (4) HNaK(1)X, (5) HNaCs(3)X, (6) HNaCs(2)X, (7) HNaRb(1)X, and (8) HNaRb(3)X.

exchanged type X zeolites. It is seen from Figure 6 that the sorption rate decreases with the increase in the degree of exchange.

Similarly Figure 6 shows that equilibrium sorption capacities at $(P/P_0 = 0.5)$ and 298 K also decrease with the increase in the degree of exchange and also with the increase in the ionic size of the exchange cation. The striking feature of Table VI is the higher sorption of benzene compared with that of n-hexane inspite of the greater molecular size of the former (5.85 Å) compared with that of the latter (4.2 Å). Benzene is comparatively spherical in shape, whereas n-hexane is cylindrical; and hence the packing of benzene is expected to be closer than that of n-hexane. At the same time, bonding offers some polarity to benzene and hence becomes cation-specific compared to only the volume filling character of almost nonpolar n-hexane. Sorption of benzene decreases from 40.2 molecules/u.c. in NaX to 36–35 molecules/u.c. in higher exchanged KX and RbX samples. Surprisingly, the benzene sorption capacity remains almost unaffected by the degree of Cs exchange. The sorption capacity of n-hexane decreases from 29.2 molecules/u.c. in NaX to 21–22 molecules/u.c. in higher alkali metal exchanged samples. It also

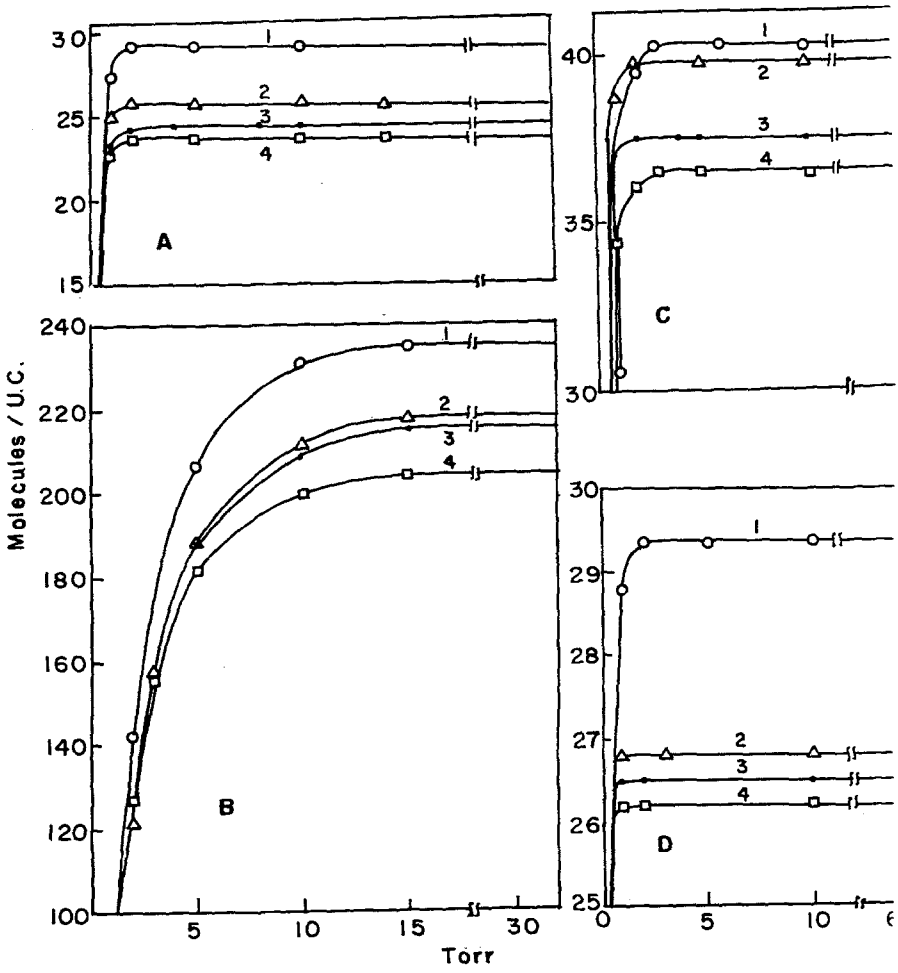

Fig. 6. Sorption kinetics for (A) n-hexane, (B) water in (1) NaX, (2) HNaK(1)X, (3) HNaK(2)X, and (4) HNaK(3)X; (C) Benzene in (1) NaX, (2) HNaRb(1)X, (3) HNaRb(2)X, (4) HNaRb(3)X, and (D) cyclohexane in (1) NaX, (2) HNaCs(1)X, (3) HNaCs(2)X, and (4) HNaCs(3)X.

decreases monotonically with the increase in the degree of exchange. The sorption of larger cyclohexane molecules (6.8 Å) and that of n-hexane (4.2 Å) is 29.3 molecules/u.c. in NaX zeolite. The sorption of cyclohexane is lower than that of benzene but decreases negligibly with the degree of exchange. The sorption of n-hexane, however, decreases monotonically with the increase in the degree of exchange. This also shows that packing of the larger but spherical cyclohexane is least affected. However, the packing of the smaller but cylindrical nonpolar n-hexane molecule seems to be affected by the introduction of larger alkali metal cations.

The sorption capacity of TMB is lower than that of benzene, cyclohexane and n-hexane. It decreases with the degree of exchange from 25.7 molecules/u.c. for NaX to about 19–20 molecules/u.c. in HNaK(3)X, HNaRb(3)X and HNaCs(3)X. This is in accordance with the larger molecular size among the sorbate molecules used.

The equilibrium sorption capacity of water in NaX is 236 molecules/u.c. and this is in close agreement with the literature value [14]. It then decreases with the degree of exchange up to 198 molecules/u.c. However, the observed decrease in the water sorption with the degree of exchange and the nature of the alkali metal cation may be due to the larger cationic size and may also be altered due to the cation distribution among the available cation sites. This is then responsible for the reduction in the available void volume. Water is sufficiently smaller in size to enter the cages and hexagonal prisms to interact with cations located therein.

Acknowledgements

Authors are thankful to Dr. P. Ratnasamy for his constant encouragement. Thanks are also due to K.S.N. Reddy for timely help.

References

1. P.B. Venuto and P.S. Landis: *Adv. Catal.* **18**, 259 (1968).
2. H.F. Leach: *Ann. Rep. Progr. Chem.* **68A**, 195 (1971).
3. D. Barthomeuf: Proc. Zeocat-90, *Catalysis and Adsorption by Zeolites*, Stud. Sur. Sci. and Catal. Vol. 65, Eds. G. Ohlmann, H. Pfeifer, and R. Fricke. Amsterdam, p. 157 (1991).
4. K.S.N. Reddy, M.J. Eapen, H.S. Soni and V.P. Shiralkar: *J. Phys. Chem.* **96**, 7923 (1992).
5. R.P. Townsend and M. Loizidou: *Zeolites* **4**, 191 (1984).
6. D. Axente, M. Abrudean, and A. Baldea: *Zeolites* **3**, 259 (1983).
7. M. Eic, M. Goddard, and D.M. Ruthven: *Zeolites* **8**, 327 (1988).
8. T. Yashima, K. Sato, T. Hayasaka, and N. Hara: *J. Catal.* **26**, 303 (1972).
9. D.W. Breck and E.M. Flanigen: *Molecular Sieves*, Soc. Chem. Ind. London, p. 47 (1968).
10. V.P. Shiralkar and S.B. Kulkarni: *Ind. J. Chem.* **16A**, 665 (1978).
11. V.P. Shiralkar: Ph.D. Thesis, University of Pune (1980).
12. R.M. Barrer, J.A. Davies, and L.V.C. Rees: *Inorg. Nucl. Chem.* **30**, 3333 (1968).
13. A.H. Badran, J. Dwyer, N.P. Evmerides, and J.A. Manford: *Inorg. Chem. Acta.* **21**, 61 (1977).
14. V.P. Shiralkar and S.B. Kulkarni: *Zeit. Phys. Chemie. Neue. Folge* **132**, 213 (1982).
15. E.M. Flanigen, H. Khatami, and H.A. Szymanski: in *Molecular Sieve Zeolites*, I, Adv. Chem. Ser. Vol. 101, Eds. R.F. Gould, Am. Chem. Soc., Washington, D.C., p. 201 (1971).
16. E. Stuckenschmidt, H. Fuess, and F. Pechar: *Phys. Chem. Miner.* **15**(5), 461 (1988).
17. J. Scherzer, J.L. Bass, and F.D. Hunter: *J. Phys. Chem.* **79**, 1194, 1200 (1975).
18. H. Bremer, W. Morke, R. Schodel, and F. Vogt: *Molecular Sieves*, Adv. Chem. Ser. Vol. 121, Eds. R.F. Gould, Am. Chem. Soc., Washington, D.C., p. 249 (1973).
19. M.M. Dubinin and I.V. Radushkevich: *Proc. Akad. Sci. USSR* **55**, 327 (1974).
20. V.P. Shiralkar and S.B. Kulkarni: *Z. Phys. Chemie, Leipzig* **265**, 313 (1984).
21. R.M. Barrer and B. Coughlan: *Molecular Sieves*, Soc. Chem. Ind. London, p. 233 (1968).
22. V.P. Shiralkar and S.B. Kulkarni: *Zeolites* **5**, 37 (1985).